Cooking Oil Based Asphalt
A Major Qualifying Project Report:
Submitted to the Faculty
of the
WORCESTER POLYTECHNIC INSTITUTE
in partial fulfillment of the requirements for the
Degree of Bachelor of Science
by

Emmanuel Michaelidis

Shane Sampson

Tory Sidoti

Date: February 29, 2013

Approved:

Professor Rajib B. Mallick

Capstone Design Experience

The Project satisfied the capstone design experience requirement by conducting an analysis and design study to determine the optimal structure of a model pavement, and the material of the layers, to obtain a desired range of tensile strain due to repeated loading. This was achieved by using a layered elastic analysis. Several structures were considered and analyzed until a desired one was obtained. The final structure was selected on the basis of several factors which included engineering consideration, manufacturability, and cost.

Abstract

This study looks at determining the suitability of waste cooking oil-based asphalt for making Hot Mix Asphalt (HMA), through structural strength testing – rutting and fatigue properties, using the South African Model Mobile Load Tester (MMLS3). Slabs of conventional and waste cooking oil asphalt mixes were tested for fatigue and rutting properties. These results showed that there was no statistical difference in rutting between the two slabs and a significant difference in fatigue testing.

Acknowledgements

The project group would like to thank their advisor Rajib B. Mallick for all the advice and guidance he gave during the project. Special thanks to Donald Pellegrino, and Russell Lang for their technical support throughout all the testing that was done for this project. Also Ryan Worsman, a graduate student concerning similar topics, for his timely help. Finally the group would also like to thank Washington State University for providing the Bio Asphalt.

Table of Contents

List of Tables

List of Figures

1. Introduction

This project is researching the theory of using used cooking oil as an added substitute for binder to produce Hot Mix Asphalt (HMA). This would help making asphalt structures more sustainable by reusing wasted cooking oil and reducing the use of asphalt. The project compared the results of rutting and fatigue testing between a control slab prepared with a conventional asphalt binder and a slab produced using "bio-asphalt" which contained cooking oil.

The data used to compare these two slabs came from two different tests. Both tests were conducted using the South African Model Mobile Load Simulator (MMLS). The first test was conducted to measure rutting at a temperature of 50 degrees Celsius, using an environmental chamber, and loading for a fixed period of time. The slab was marked off into ten even sections and the rut depths were measured on the left, middle and right areas of the wheel path. The second test was a fatigue test where the resulting tensile strain at the bottom of the slab was measured using strain gauges. These strain gauges were attached to the slab, using epoxy. The strain cages were then connected to a data acquisition system, which was used to collect the data through a computer.

The key to getting comparable data from these two slabs was to create them in identical ways. The form in which the HMA was to be poured in and compacted in had to be the same, the mixing and compaction processes needed to be uniform and the testing procedures for rutting and fatigue needed to be equivalent so that similarities or differences could be conclusively defined.

2. Objectives

The objectives of this project were to design a structure of the model pavement in the laboratory that would provide the desirable range of strain data for fatigue analysis. Also to provide a mean rut depth that is adequate for structural use.

3. Literature Review

3.1 Literature Review Summary

The world today is searching for ways to create more sustainable infrastructure and goods. With many construction projects requiring nonrenewable materials while also emitting harmful bi-products, researchers are trying to develop ways to reuse waste products in the production process. With 96% of the roadways in the United States surfaced by asphaltic materials, there have been investigations into the use of waste materials in asphalt production, and specific to this project is the use of used cooking oil. This idea of creating more sustainable asphalt would look to replace the method of using tars and toxic oils, which can be very harmful to the environment. This project will first test for the permanent deformation, or rutting, that occurs when a wheel path passes over the asphalt (pg158 (1)). It will also compare the results of fatigue of bio asphalt and control petroleum asphalt. The fatigue test, conducted using strain gauges, will reveal the moment of strain at which the pavement will fail.

3.2 Current Pavement Disadvantages

The current material makeup of asphalt has many disadvantages, the major one being its harmful effects on the environment. In a 2010 study, *The Influence of Different Urban Pavements on Water Chemistry*, found "pavements are a potential source of multiple pollutants but it remains unclear as to whether these pollutants would be sequestered in the soil or delivered to receiving waters" (2). If sequestered in the soil, this could affect the growth of vegetation as these pollutants can deplete the nutrients plants use to grow. If these pollutants are delivered to receiving waters they can affect the wildlife that inhabit the water bodies as well as affect animals that rely on the waters as a source of drink. This polluted water can also include reservoirs that supply drinking water for humans. Another disadvantage to petroleum based

asphalt is that the price of refined oil continues to climb. “Increased environmental regulations for new drilling, dwindling existing resources, modifications to the refining process that maximize the fuel quantity while minimizing asphalt residue have increased the cost of asphalt in recent years” (3).

3.3 Bio Asphalt

Although scientists have created different forms of bio asphalts, the one used in our project is made from used cooking oil. In 2011, The Environmental Protection Agency reported that in the United States alone, approximately 3 billion gallons of waste cooking oil is collected annually. The use of this waste product diverts used cooking oil from making its way to landfills and sewer pipes and coverts it into an energy source (4). “Oils and grease may cause the clogging of the pipes because they stick to the inner walls and reduce the effective diameter of the sewer pipes. If this layer becomes thicker, it may cause sewage spills” (5). Using waste cooking oil as an additive for producing HMA is inexpensive and very environmentally beneficial. This project uses a sample of waste cooking oil collected by the University of Washington State University of which was blended with a conventional PG 64-22 binder at 10% of the total weight of the conventional binder.

3.4 Pavement Rutting

When a pavement is said to “rut” it is subject to a permanent deformation from a load of a wheel path over the asphalt. Asphalt can be subject to two basic types of rutting; mix rutting and subgrade rutting. “Mix rutting occurs when the subgrade does not rut yet the pavement surface exhibits wheel path depressions as a result of mixing/compaction problems. Subgrade rutting occurs when the subgrade exhibits wheel path depressions due

to loading. In this case, the pavement settles into the subgrade ruts causing surface depressions in the wheel path" (6). Mix design rutting can be caused by unstable mix design, heavy vehicle traffic, and/or high pavement temperatures. The most common places that these ruts can be seen are at intersections, or places that have continuously heavy loading, such as bus stations. A mix rut can be seen in Figure 2 below. Subgrade rutting is caused by an overstressing of the layers beneath the asphalt surface, or subgrade. It can be due to insufficient thickness for the areas traffic conditions or insufficient strength in the underlying materials. Moisture which finds its way into the subgrade can have a weakening effect on the pavements material make-up and applied loading from traffic can inflict permanent deformation (7). An example of subgrade rutting can be seen in Figure 1.

Figure 1: Rutting

A pavements ability to withstand loads and not let rutting occur is very important as it increases its lifetime and increases traffic safety. When a rut occurs it forms a trough like structure and when filled with water can increase the likelihood of hydroplaning.

Figure 2: Water collecting in ruts

3.5 Pavement Fatigue

Testing for pavement fatigue can be very useful in determining the life span of designed hot mix asphalt. When a load is placed on a pavement it experiences strain, or a tensile force, which usually occurs on the bottom of the grade. If the pavement experiences a low strain then it may not experience fatigue but it the strain is high enough, depending on a given mix design and loading, fatigue failure may occur. When the pavement fails it will result in fatigue cracking, which can lead to deterioration of the materials (10). An example of fatigue cracking can be seen in Figure 3.

Figure 3: Fatigue cracking

An important factor in the mix design of pavement to avoid fatigue failure is its percent air voids. The general rule of thumb for percent air voids is 6-7% and as the air voids increase there is a trend in the reduction of fatigue life. “Too high an air void content provides passageways through the HMA for the entrance of damaging air and water. Too low an air void content, on the other hand, may lead to flushing, a condition where excess binder squeezes out of the HMA to the surface” (11). It is important to design a pavement correctly suited for environment that it will be used as fatigue failure can be a hard to manage and very costly.

4. Scope of Work

The plan involved a series of steps that had to be followed precisely in order to make this experiment valid. The initial step was to develop a gradation analysis of the types of aggregates that were being used for the asphalt slabs, which included: 1/2” stone, 3/8” stone, stone dust, and natural sand. The initial sieve analysis of the cumulative percent retained can be seen in the Table 1 below.

Table 1: Cumulative Percent of Aggregates Retained in Sieves

		Cumulative Percent Retained									
Size (in)	Size (mm)	Stone Dust	Natural Sand	3/8	1/2	Design	JMF	Lower Limit	Upper Limit	% Stone Dust	22.5
5/8	15.75	0	0	0	4.633	0.3	0	0	0	% Natural Sand	20
1/2	12.5	0	0	0	66.259	5.0	1	0	5	% 3/8 Stone	50
3/8	9.51	0.0	0.2	0.0	94.347	7.1	7	0	20	% 1/2 Stone	7.50
#4	4.75	1.0	3.3	72.1	99.24	44.4	41	24	50		
#8	2.36	17.2	6.8	97.6	99.24	61.5	57	51	63		100
#16	1.18	39.9	12.6	97.9	99.24	67.9	70	60	74		
#30	0.6	62.3	25.6	98.0	99.24	75.6	79	71	83		
#50	0.3	78.1	56.0	98.2	99.24	85.3	86	79	90		
#100	0.15	90.1	88.2	98.4	99.24	94.6	91	84	95		
#200	0.075	94.6	95.4	98.8	99.24	97.2	96	93	98		
Pan	Pan	100.0	100.0	100.0	100.0	100.0	100	100	100		

The various aggregates were combined in the appropriate proportions to obtain the desired gradation of a MADOT surface course. This gradation was used with the optimum asphalt content (6%) to produce mixes, which were first tested for Theoretical Maximum Density (TMD). The results are shown in Table 2.

Table 2: Theoretical Maximum Density of Slab Mix Design

Sample ID	Bag Weight (g)	Weight of Rubber (g)	Weight of Sample in Air (g)	Weight of Sample Submerged (g)	(A+B+C)-D Total	A/Vc + B/Rc	E-F Sample	C/G Density
A	72.7	0	1962.1	1141.5	893.3	80.48267464	812.8173254	2.413949529
B	74.4	0	1927.8	1112.2	890	82.3646629	807.6353371	2.386968365
C	74.3	0	1957.1	1133.8	897.6	82.25395771	815.3460423	2.400330533
D	73.3	0	1959	1142.6	889.7	81.14690579	808.5530942	2.422846457
						A,B,C,D -->	Avg TMD	2.406023721

4.1 Slab Construction

This project involved rolling two slabs using two different types of asphalt binder, one using PG 64-24 asphalt binder while the other used cooking oil based binder that was provided by Washington State University. The two different slabs were built in a mold that was 3’ x 3’ x 4”, then cut in half to create two separate slabs for the tests that were performed. Thus, a total of four slabs were made with the two different asphalt binders. Then, four other molds were designed, each 3’ x 1.5’ x 4”, to house the four slabs for rutting and fatigue testing. All the molds were made out of wood and were designed so they would withstand the load of the MMLS machine without letting the slabs shift in any way to allow a continuous straight tire path on the slab which made sure the data we obtained was accurate.

4.2 Tests Performed

Two tests were done in order to test the rutting and fatigue properties of the two different slabs. Therefore, a total of four tests were done over the course of the project; two tests for each slab.

The rutting test was conducted for an 8-hour period with the MMLS machine running at ¼ of its maximum speed. At full speed the MMLS applies 7,200 pound load application per hour. The loading comes from four tires which are inflated to 100 psi. Then the depth of the rut, for each the control slab and the bio asphalt slab, was measured by using a straight edge and calibrator. The rut was measured three times in ten different sections of the tire path; the three measurements were taken from the left side, middle, and right side of the tire path. Therefore, a total of thirty measurements were taken over the course of one slabs tire path.

The fatigue test was conducted over the course of a one week period with the MMLS machine running at full speed, with a tire load of six-hundred and seven pounds. Each slab was

instrumented with a total of five strain gages at the bottom of the slab, three positioned longitudinally and two positioned transversely. These gages were soldered to individual wires that were then attached to a data acquisition system which used Lab View to record the strain values. Six inches of D60 neoprene was placed under the slab: in the mold. This was done to obtain the most optimal strain during fatigue testing. The collected data was later analyzed.

4.3 Flow Chart of Test Plan

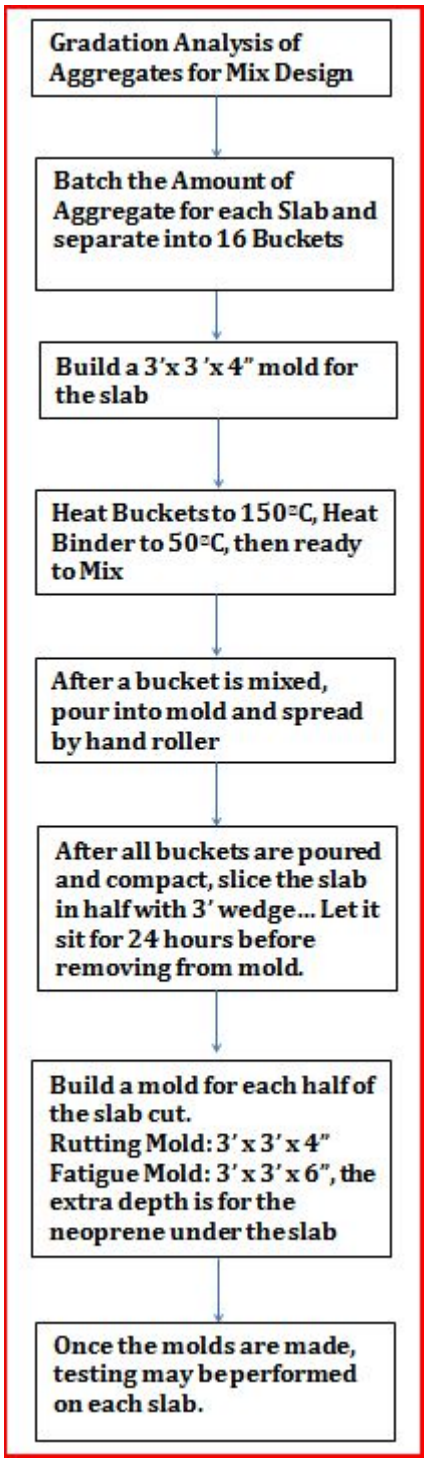

Figure 4: Flow Chart of Test Plan

5. Experimental Work

5.1 Details of Slab Preparation for Fatigue Tests

The objective of the fatigue testing was to have the slab fail and to do this the project team needed to produce between 150 and 400 micro strain. To ensure this, the modulus of elasticity €, Poisson ratio ν, and correct thickness of each layer in the slab mold had to be acquired to predict the resulting strain with the given load. The team decided to use a 4 inch layer of Neoprene type 60D because it had a low modulus of elasticity. The strain was calculated using a program called WinJULEA, after inputting the thicknesses, modulus of elasticity's, and Poisson's ratio for each material, as well as the force of the tire of the MMLS and the depth at which the strain gauges would be placed. Figure 5 shows an output from the layered elastic analysis to determine the optimum structure.

Untitled

*** LAYERS STRUCTURE

LAYER NUMBER		THICKNESS	MODULUS OF ELASTICITY	POISSON RATIO	INTERFACE CONDITION
1	HMA	3.70	350000.00	0.35	0.00
2	Neoprene	4.00	11.82	0.49	0.00
3	Wood	0.75	1318000.00	0.34	0.00
4	Steel	0.50	28985000.00	0.27	0.00
5	Concrete		3625000.00	0.15	

*** APPLIED LOADS

LOAD NUMBER	X COORD	Y COORD	LOAD MAGNITUDE	CONTACT AREA
1	0.00	0.00	607.00	6.07

*** EVALUATION POINTS

POINT NUMBER	X COORD	Y COORD
1	0.00	0.00

*** CALCULATION DEPTHS

DEPTH NUMBER	DEPTH
1	3.69

*** RESULTS

STRAIN-X	STRAIN-Y	STRAIN-Z
-0.150E-03	-0.150E-03	0.162E-03

Figure 5: WinJULEA report

5.2 Molds

While the aggregates were heating up, the project team assembled the mold. The dimensions desired for the project by the advisor where 3'x3'x4". For this the project team gathered two 4"x6' boards and plywood. The boards where cut in half and drilled onto the plywood to create a 3'x3'x4" mold to which the HMA will be applied. Half of the mold (1.5'x3'x4") was designed for the fatigue test and the other half for the rutting test.

For the fatigue side of the mold, half inch imprints for transverse and longitudinal strain gages were made by epoxying metal wire and ceramic rectangles onto the mold. These gages must be equidistant and in the center of the fatigue slab. The transverse gages needed the metal wire to go 7.5" into the slab and the longitudinal gages needed a metal wire with the distance of 9.5", placing both in the direct center of the slab. Once the metal wires were placed the ceramic rectangles were epoxied respectfully, either transversely or longitudinally. The photograph in Figure 6 below shows a close up of the imprints on the mold.

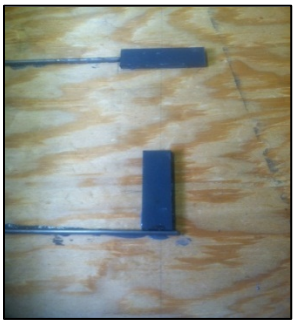

Figure 6: Strain Gage Imprint

The rutting side of the mold was easier to assemble. It did not need anything done it just needed to be flat. Once the mold was complete the project team layered it with aluminum foil, which prevents the HMA from sticking to the mold. The HMA is then ready to be poured.

5.3 Mixing

The aggregates and binder were heated up in the oven to reach a temperature of 150 C. The project team also heated up the mixing blade and the roller to allow smooth mixing and compacting. The correct calculated weight of binder was added to each bucket of aggregate. This occurred one bucket at a time to keep the other buckets warm in the oven. Once the correct amount of binder was added to the aggregate the project team started to mix the bucket using the motorized rotational bucket mixer. Once the bucket was mixed it was placed back into the oven and a new bucket of aggregate was removed from the oven. The process was repeated until all buckets where properly mixed, and they were left in the oven for about 10 minutes to allow them to heat up one last time before pouring. Photos from this process can be seen in Figures 7 and 8 below.

Figure 7: Left: Binder being added to aggregate; Right: Mixing the binder and aggregate

Figure 8: Aggregates and binder heating in oven

5.4 Pouring

For the pouring process the project group needed a handful of tools including; a heated roller, soapy water and a brush, rake, and a tamp. While dumping the HMA into the mold one member of the group used the rake to spread it evenly while the others used the roller to compact it. The soapy water was used on the roller so the HMA would not stick to it. Finally, the tamp was used to level the compacted HMA at the end of the pouring.

After pouring was complete, a blade was hammered into the middle of the asphalt using two sledgehammers to split the slab in half. This allowed the group to acquire its rutting and fatigue slabs. The final product can be seen in the Figure 9 below.

Figure 9: Left: Conventional asphalt slab; Right: Bio-asphalt slab

5.5 Rutting

Once the HMA was properly cooled the project team moved onto the rutting test. After separating the slab, the team created a new mold, with dimensions 3'x1.5'x4", to fit the rutting slab in. Using the overhead crane the slab was moved to the Model Mobile Load Simulator (MMLS) mold. The slab was placed in the direct center of the mold so an even load distribution occurred across the entire slab. In order to accomplish this, the project team first modified the original slab mold so that it would be able to contain the control slab; this can be seen in Figure 10 below.

Figure 10: Mold for conventional slab

Once the mold control slab was placed in the correct spot, reinforcements were placed in the four corners of the mold to ensure the mold was stabilized during testing. To accomplish this task, four 2”x 6” pieces of lumber were wedged from the end of the pathway to the separate corners of the mold. After this step was complete, the MMLS3 was placed over the center of the mold. To do this the project team used the overhead winch to lift the machine over the mold and then locked it into place with its built in frame. An image of this process can be seen in Figure 11 below.

Figure 11: MMLS machine positioned over control slab

When the MMLS was secured to the frame, the tire pressure along the surface of the slab was checked to make sure that it was between 90-100 psi. The environmental chamber was then placed over the MMLS machine to encase the whole slab. The environmental allows heat vents to be placed through slits on the two sides. The entire procedure of this can be seen in Figure 12 below.

Figure 12: Left: Environmental Chamber being lowered over slab; Right: Heating vents

The heating vents were secured by use of zip ties around the pipes where they were attached to prevent any heat from escaping. The temperature of the ventilation system was set to 50 ˚C and the slab was heated up for approximately twelve hours before testing begun.

When the test ended the rut depth of the slab was measured by dividing the slab into ten increments, seen in Figure 13 below, and three separate measurements were taken on each of the ten sections of the rut. The measurements were done by using an electric caliper that could accurately take measurements.

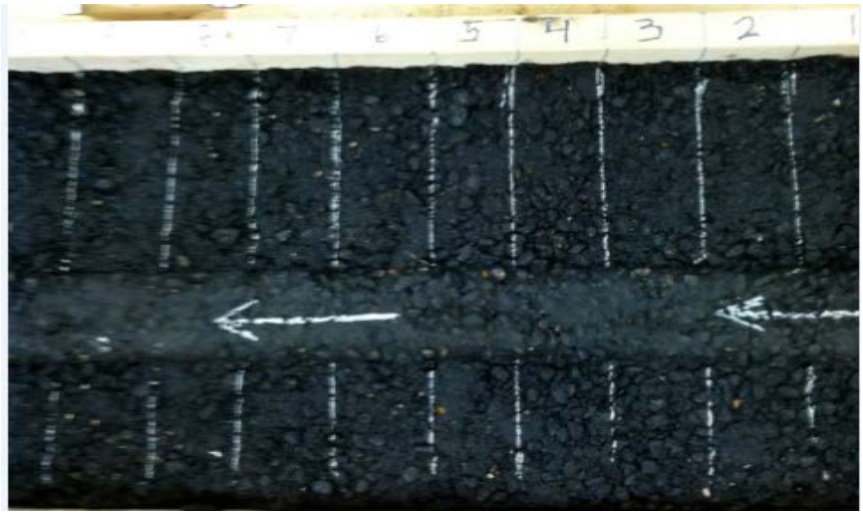

Figure 13: Slab divided into ten increments to measure rut

5.6 Fatigue

For the fatigue test the MMLS needed to be run at full speed (approximately 7,200 repetitions per hour) at room temperature (25° C) until the strain gages failed. Before the fatigue testing started the project team needed to make sure that the maximum strain would be between 150 and 400 micro strain. In order to achieve this, the team needed to figure out what materials and thickness could be used to achieve this quantity of strain. This step is described earlier in Details of Slab Preparation for Fatigue Tests.

The materials decided upon to include in the mold were neoprene, and wood. The steel base of the MMLS and the concrete floor where also accounted for. A schematic of the final structure used for fatigue testing is shown in Figure 14.

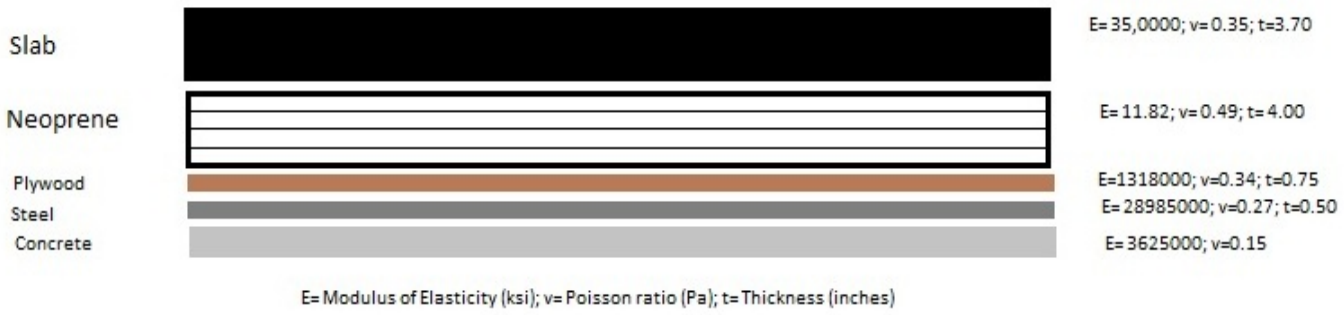

Figure 14: Final layered strain design

5.7 Preparation of Fatigue Slab

First, the strain gages were attached at the bottom of the slab using epoxy. As the epoxy cured the other parts of the new mold were put together. Using the results of the analysis and design ¾ of an inch of plywood made the base and four inches of Neoprene D60 were placed on top of that. One the epoxy cured, the slab was carefully placed on top of the neoprene, and with

all edges flush, the 3’ x 1.5’ x 9” wooden border was added. The nine inch sides were needed to enclose the five inches of wood and neoprene and the four inch slab. Before securing the sides, holes were drilled in one side to allow for the wires of the strain gages to come through. Figure 15 below illustrates the fatigue slab preparation.

Figure 15: Left: Imprints in slab for strain gages; Right: Strain gages epoxied onto slab

Once the mold was completed the slab was moved and positioned into the center of the MMLS. This slab, like the rutting slab, was braced by wood to insure that it would not move during testing. When the slab was finally braced, the MMLS was placed over the slab. Figure 16 shows a photo the fatigue slab under the MMLS.

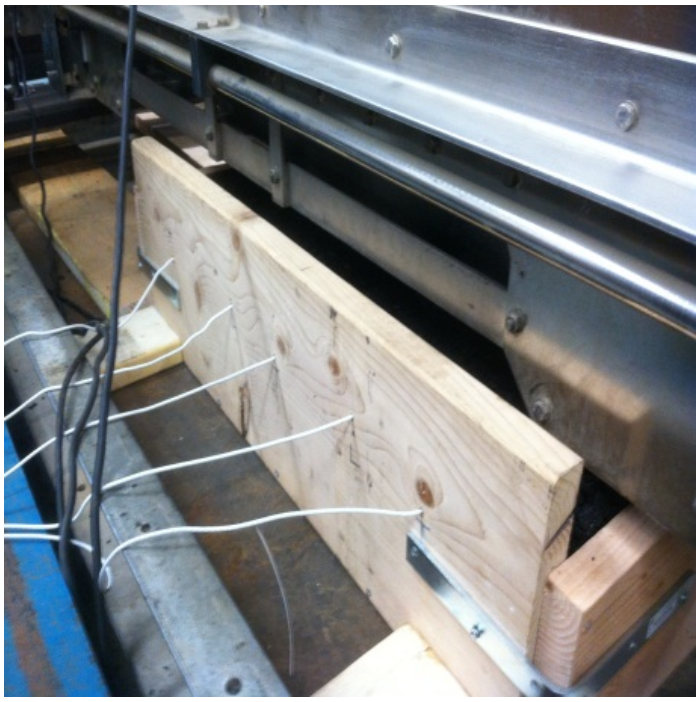

Figure 16: Fatigue slab under MMLS machine

When the MMLS was secured to the frame, the tire pressure along the surface of the slab was checked to make sure that it was approximately 690 KPa. The strain gage wires were then inserted into the computer and LabView software was started to read the data from the gages. Figure 17 shows an example of the strain data being collected in LabView.

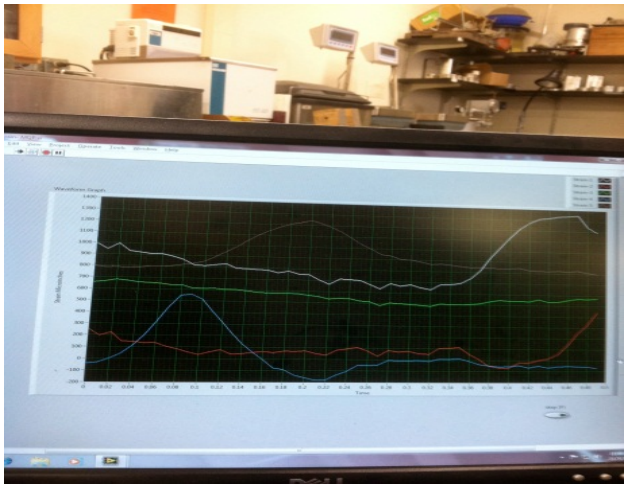

Figure 17: LabView reading data from strain gages

5.8 Cores Samples

Core samples were obtained from the slabs to determine the percent air voids. A total of six core samples were drilled out of each slab. Three cores where taken from the rutted tire path of each slab and three more from the side that was not affected by the MMLS.

6. Experimental Results

6.1 Rutting Control Test

The control slab was under the MMLS machine for 12 hours with a speed of about 286 load revolutions/hour, as seen in section 9.2 of the Appendix. Table 3 shows the rut depth data. Figure 18 is a graph showing the rutting measurements.

Table 3: Control Slab rut depth data

Measurement (mm)	1	2	3	4	5	6	7	8	9	10	AVG	Total Avg
Left Outside	16.8148	16.637	12.6746	10.8458	10.9982	8.9916	10.5664	13.2588	17.018	21.6154	13.94206	14.70152
Middle	20.9804	19.2278	16.129	13.6398	16.1036	13.0048	13.1064	15.2654	18.4912	22.9108	16.88592	
Right Outside	16.129	15.24	11.9126	11.176	11.4808	11.2014	11.6586	12.8524	13.8684	17.2466	13.27658	

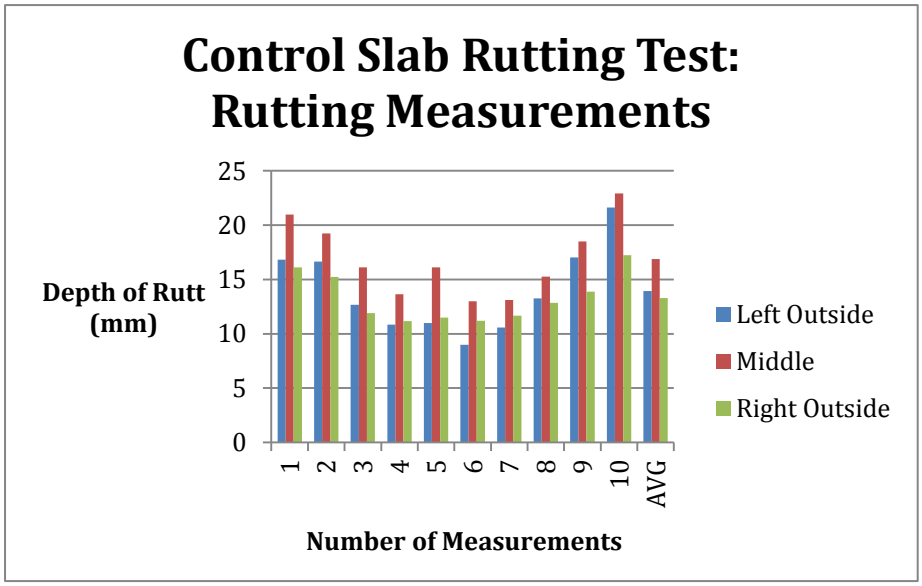

Figure 18: Control slab rutting measurements graph

The average for the left outside was 13.94 mm, the middle 16.88, and the right outside 13.28. The total average depth was 14.7 mm, just about 2mm deeper than the target. As expected the measurements in the middle of the rutting where larger than the measurements taken from the outsides for all increments.

6.2 Bio Asphalt Slab Rutting

The Bio Asphalt slab was under the MMLS machine for 8 hours while running at a speed of approximately 286 revolutions/hour when the project team noticed a rut of approximately 12.5 mm, seen in section 9.2 of the Appendix. Table 4 shows the rut depth data. Figure 19 is a graph of the rutting measurements.

Table 4: Bio-asphalt slab rut depth data

Measurement (mm)	1	2	3	4	5	6	7	8	9	10	AVG	Total Avg
Left Outside	13.3	12.3	10.1	13.1	9.6	10	11.4	16.5	20.6	22.4	13.93	15.28333
Middle	14.4	14.8	14.9	15	13	13.2	17.5	23	22.9	27.2	17.59	
Right Outside	10.9	11.8	11.6	13.1	8.9	11.6	16.2	15.3	23.4	20.5	14.33	

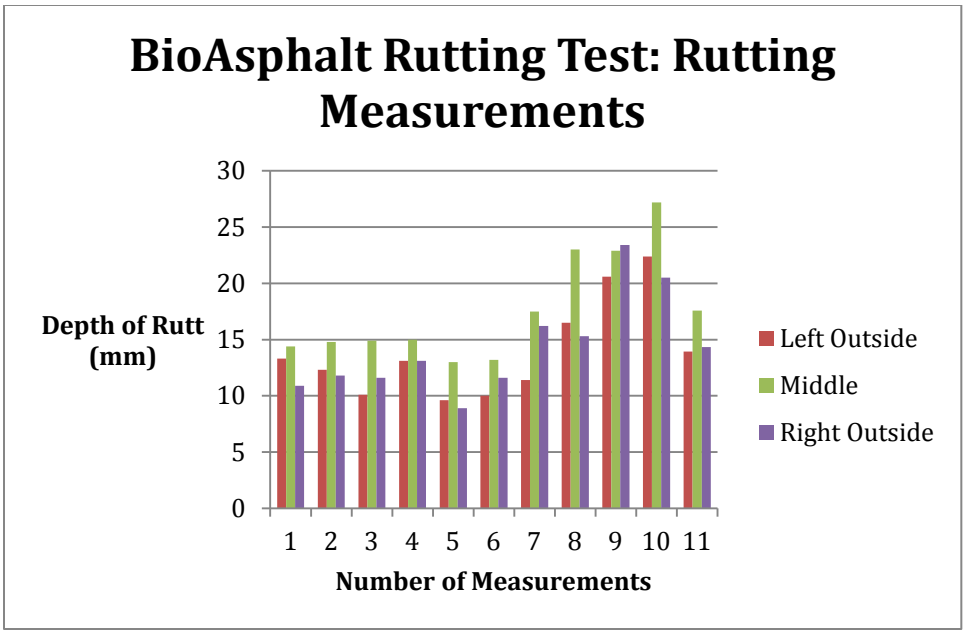

Figure 19: Bio-asphalt rutting measurements graph

The average for the left outside was 13.93 mm, the middle 17.59, and the right outside 14.33. The total average depth was 15.283 mm, just about 3mm deeper than the target. As expected the measurements in the middle of the rutting where larger than the measurements taken from the outsides for all increments. The Bio Asphalt slab was tested 4 hours less than the Control slab and had more rutting.

6.3 Control Slab Fatigue Results

The control slab was tested under the MMLS machine for approximately five and a half days before four of the gages had failed. A MatLab code was developed in order to see the strain in tabular and graphical form; samples of these visuals may be seen in section 9.3 of the Appendix. In order to find where the gages failed, MatLab was used to find the maximum strain of each gage per 12 hours of testing, or approximately 4,320,000 cycles of the MMLS machine. This was done until a significant change was identified in the data,

which was where the gages failed; these can all be seen in section 9.3 of the Appendix. Photos of the cracking in the control slab can be seen in section 9.3 of the Appendix.

6.4 Bio Asphalt Fatigue Results

The Bio Asphalt slab was tested under the MMLS machine for approximately ten days until two of the gages had failed; additional testing was done to attempt and fail the other gages but after eleven days of total testing gage 2, 3, and 4 were unable to fail. Similar to the Control Slab Fatigue data, a MatLab code was developed in order to see the data in tabular and graphic form; these can be seen in section 9.3 of the Appendix. Maximum strain values were found for each twelve hour set of data, or approximately 4,320,000 cycles. This process was continued until a significant change in strain occurred. These gage failures can be seen in section 9.3 of the Appendix. Photos of the cracking in the bio asphalt slab can be seen in section 9.3 of the Appendix.

7. Analysis

7.1 Statistical Analysis of Rut Depth Data

After completing the statistical analysis it was found that the mean rut depth for the middle of the tire path for the control slab was 16.88mm and 17.59mm for the bio asphalt slab. The standard deviation for the control slab was 3.41mm and 4.97mm for the bio asphalt slab.

An F test was conducted to calculate the following: A null hypothesis stating that there is no significant difference in rut depth, and an alternative hypothesis stating that there is a significant difference in the rut depth. The results of this hypothesis are shown in table 5. As can be seen, the F calculated is not greater than or equal to the F critical. Hence, the conclusion is

that the null hypothesis cannot be rejected. Therefore, it can be concluded that the mean from the two slabs are not significantly different.

Table 5: Rut statistical analysis values

Source	SS	DF	MS	F
Treatments	2.535	1	2.535	.1396< 4.4138
Error	326.94	18	18.163	
Total	3259.5	19		

7.2 Fatigue Data Analysis

After all testing was analyzed for the Control and Bio Asphalt slab, it can be concluded that the Bio Asphalt slab was stronger than the Control slab. The reason is simply because the Bio Asphalt was able to with stand the same load and rate of loading as the Control slab for a longer period of time. The amount of strain on each of the slabs was similar in comparison can be seen in Table 6 and 7 below.

Table 6: Control Slab Fatigue Data Analysis

	Control Slab Fatigue Data (micro strain)					
	Time (about 12 Hr. Increments)	Gage 1	Gage 2	Gage 3	Gage 4	Gage 5
Day 1	1-4,320,000 Cycles	1022	948	836	925	725
	4,320,000 - 8,640,000 Cycles	911	785	754	890	670
Day 2	8,640,000-12,960,000 Cycles	628	584	504	615	428
	12,960,000-17,280,000 Cycles	601	474	451	563	351
Day 3	17,280,000-21,600,000 Cycles	573	496	423	473	315
	21,600,000-25,920,000 Cycles	556	317	352	497	324
Day 4	25,920,000-27,387,532 Cycles	555	444	383	424	341
	1-4,320,000 Cycles	2398	3353	2119	2184	3759
Day 5	4,320,000 - 8,640,000 Cycles	0.349	-4124	1430	3923	3759
	8,640,000-12,960,000 Cycles	-7.84	-4124	1520	-4115	-4273
Day 6	12,960,000-16,881,297 Cycles	5.85	-4124	1228	-4115	-4273
	End of Test					

Table 7: Bio Asphalt Fatigue Data Analysis

	Bio Asphalt Fatigue Data (microstrain)					
	Time (about 12 Hr. Increments)	Gage 1	Gage 2	Gage 3	Gage 4	Gage 5
	1-4,320,000 Cycles	991	401	836	880	997
Day 1	4,320,000 - 8,640,000 Cycles	526	305	743	732	684
	8,640,000- 12,960,000 Cycles	536	200	N/A	652	629
Day 2	12,960,000-17,280,000 Cycles	N/A	109	N/A	570	557
	1-4,320,000 Cycles	721	640	585	648	508
Day 3	4,320,000 - 8,640,000 Cycles	674	600	536	595	439
	8,640,000- 12,960,000 Cycles	648	580	522	585	442
Day 4	12,960,000-16,920,068 Cycles	653	569	510	574	445
	1-4,320,000 Cycles	543	473	472	522	407
Day 5	4,320,000-8,640,000 Cycles	607	547	499	683	425
	8,640,000- 12,960,000 Cycles	592	529	441	511	357
Day 6	12,960,000-16,646,801 Cycles	570	490	438	511	359
	1-4,320,000 Cycles	561	481	425	512	352
Day 7	4,320,000-8,640,000 Cycles	608	563	480	546	390
	8,640,000-12,960,000 Cycles	648	588	604	599	444
Day 8	12,960,000-16,782,587 Cycles	753	655	615	836	612
	1-4,320,000 Cycles	674	611	554	634	472
Day 9	4,320,000-8,640,000 Cycles	3765	618	565	644	3557
	8,640,000-12,960,000 Cycles	-1	-80	-130	-52	-258
Day 10	12,960,000-15,823,119 Cycles	-3	-76	-132	-61	-259
Day 11	1-4,320,000 Cycles	9	-81	-167	-58	-254

These tables show the similar values in strain, and significant difference in when each gage failed for each of the slabs. Figures in section 9.3 of the Appendix, show the number of repetition when each slab failed. The method adapted to select the failure point is by the identification of the maximum strain prior to the gage failing.

7.3 Density of Cores for Air Voids

After the tests were completed, cores were taken from the sides, as well as on the wheel path, from each slab. The Bulk Specific Gravity (BSG) of the cores was determined and the air voids were calculated on the basis of Theoretical Maximum Density (TMD). The BSG's, TMD's and air voids are shown in Table 8.

Table 8: BSG and Air Void Data Analysis

Sample ID	J Bulk specific gravity B/I	Air Voids	Average Air Voids
CR pre 1	2.295	4.4	
CR pre 2	2.319	3.4	4.1
CR pre 3	2.291	4.6	
CR post 1	2.312	3.6	
CR post 2	2.316	3.5	4.2
CR post 3	2.269	5.4	
CF pre 1	2.241	6.6	
CF pre 2	2.291	4.6	5.7
CF pre 3	2.261	5.8	
CF post 1	2.267	5.5	
CF post 2	2.263	5.7	6.9
CF post 3	2.171	9.5	
BR pre 1	2.134	11.1	
BR pre 2	2.114	11.9	11.3
BR pre 3	2.136	11.0	
BR post 1	2.010	12.6	
BR post 2	2.143	10.7	11.6
BR post 3	2.122	11.6	
BF pre 1	2.057	14.3	
BF pre 2	2.050	14.6	14
BF pre 3	2.083	13.2	
BF post 1	2.115	11.9	
BF post 2	2.110	12.1	12.4
BF post 3	2.086	13.1	

Control Pre-test Average:
4.88
SD: 1.13

Control Post- test Average:
5.55
SD:
2.175

Bio Asphalt Pre-test Average:
12.65
SD: 1.58

Bio Asphalt Post-test Average:
12
SD: 0.83

7.4 Pre-Testing Voids

Pre-testing voids refer to voids from the cores that were taken off the wheel path. The average pre-testing voids from the control slab was found to be 4.88 with the standard deviation of 1.13. For the bio asphalt slab the average pre-testing voids was 12.65 with the standard deviation of 1.58.

7.5 Post-Testing Voids

Post- testing voids refer to voids from the cores that were taken from the wheel path. The average post-testing voids from the control slab was found to be 5.55 with the standard deviation of 2.175. For the bio asphalt slab the average post-testing voids was 12 with the standard deviation of 0.83. Figure 20 shows a diagram of the pre and post-test core locations.

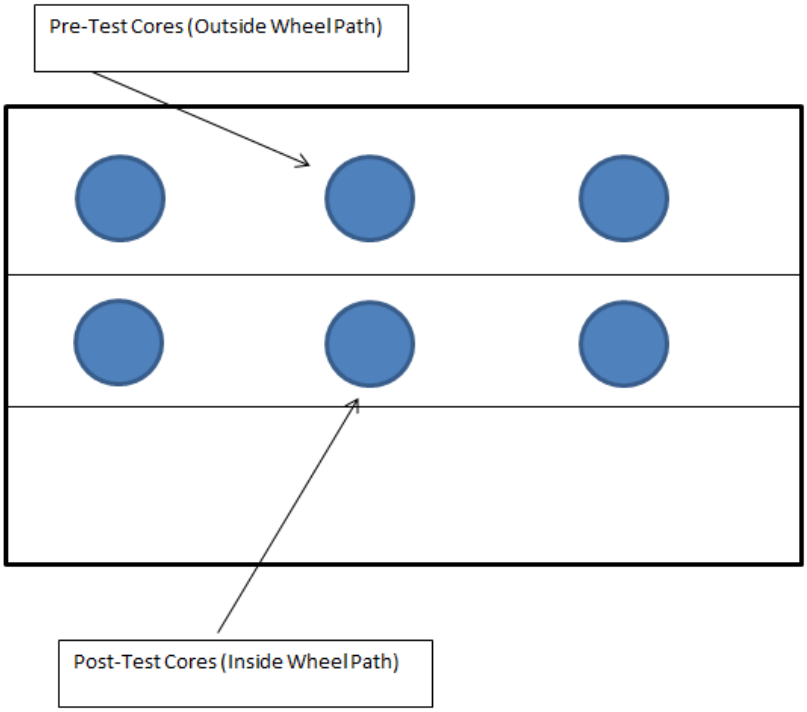

Figure 20: Locations of Cores on Slab

8. Conclusions and Recommendations

1) Based on the experimental results and analysis it can be concluded that there was no significant difference in rutting depth between the two slabs. However the fatigue analysis showed the bio asphalt l slab was less vulnerable to failure due to strain from the constant loading by the MMLS machine.

2) If this project is to be reproduced or expanded, the following recommendations should be taken into consideration. When the asphalt slabs were compacted, the project team used a manual roller. Though it did its job of compacting the asphalt evenly the project group believes that if an industrial roller was used it would have been easier to have achieved a slab of the desired design.
3) For the rutting test the group ran the MMLS until a 12.5mm rut was acquired. If future testing was to be conducted they recommend running the test for the same period of time for both slabs, instead of trying to reach a target depth. This would allow for a more exact comparison of the control and bio asphalt slab.
4) When testing the fatigue for both slabs the biggest problem the group encountered was transferring the data from LabView to MatLab to portray it graphically. The data was so large that it would not read in Excel and the group had to utilize an expert in the field in order to obtain the data in a graphical and tabular form. In the future the group recommends stopping the test for a minute and starting a new LabView file for every single day of testing. This allows for the data to be separated and analyzed in smaller files and makes it easier to import into Excel or MatLab.
5) Even though the bio asphalt was able to sustain a constant loading for a longer period of time than the control slab, the bio asphalt data showed a high void content. With a higher percent air void, the bio asphalt would be more susceptible to freezing and thawing, as well as material breakdown; therefore, causing it to be more vulnerable to fatigue cracking in certain environments.

The team recommends further testing to confirm the results of this study.

References

1. Mohammad, Louay Nadhim. *Performance Tests for Hot Mix Asphalt (HMA)*. Vol. 1469. ASTM International. Digital file.
2. Bernot, Melody J. *The Influence of Different Urban Pavements on Water Chemistry*. Taylor & Francis, 2010. Vol. 12 of *Road Materials and Pavement Design*. Digital file.
3. Wen, Ben. *Laboratory Evaluation of Waste Cooking Oil–Based Bioasphalt as*. Washington State University, 2012. PDF file.
4. "Learn About Biodiesel." *www.epa.gov*. Environmental Protection Agency, 4 Aug. 2004. Web. 22 Feb. 2013. <http://www.epa.gov/region9/waste/biodiesel/questions.html>.
5. Lapuerta, Magn. *Diesel particulate emissions from used cooking oil biodiesel*. 4th ed. Elsevier Ltd., 2008. Vol. 99 of *Bioresource Technology*. Digital file.
6. Interactive, Pavement. "Rutting." *Pavement Interactive*. Pavia Systems, 6 May 2008. Web. 22 Feb. 2013. <http://www.pavementinteractive.org/article/rutting/>.
7. Santucci, Larry. *Technology Transfer Program*. N.p.: Institute of Transportation Studies, n.d. *Techtransfer*. Web. 22 Feb. 2013. <http://www.techtransfer.berkeley.edu/techtopics/2001techtopics.pdf>.
8. Interactive, Pavement. "Flexural Fatigue." *Pavement Interactive*. Pavia Systems, 6 May 2008. Web. 22 Feb. 2013. <http://www.pavementinteractive.org/article/rutting/>.
9. *Mix Design*. N.p.: State of Indiana, n.d. *www.in.gov*. Web. 22 Feb. 2013. <http://www.in.gov/indot/files/chapter_04(4).pdf>.

9. Appendix

9.1 Slab Design

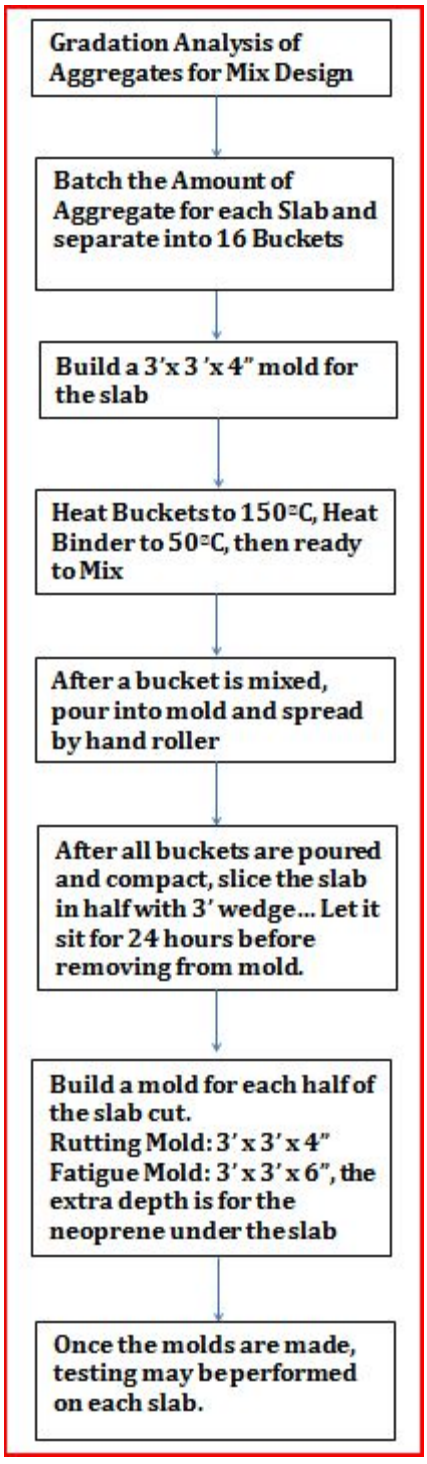

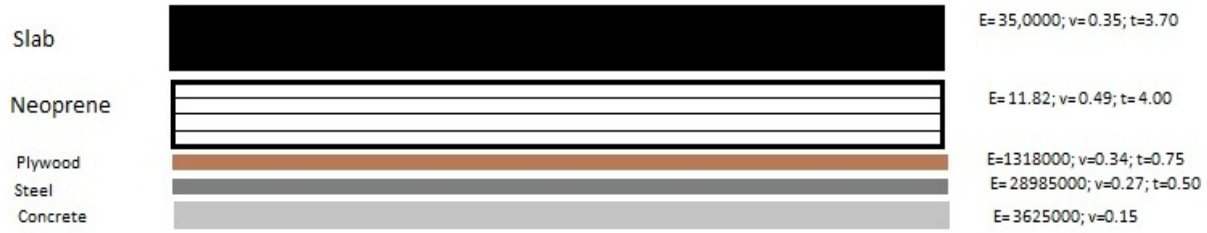

E= Modulus of Elasticity (ksi); v= Poisson ratio (Pa); t= Thickness (inches)

9.2 Rutting Analysis

Sample (mm)	Conventional	Bio Asphalt						
1	20.98	14.4						
2	19.2	14.8						
3	16.1	14.9						
4	13.6	15						
5	16.1	13						
6	13	13.2						
7	13.1	17.5						
8	15.3	23						
9	18.5	22.9						
10	22.9	27.2						
mean	16.88	17.59						
Ti, Total	168.78	175.9				T	344.68	Mean
r	10	10				N	20	17.234
sd	3.41	4.97						
SST	2.53472							
s2all	17.34080421							
dfall	19							
TSS	329.47528							
SSError	=TSS - SST							
	326.94056							

Control Slab Cycles

Date	Time	HMA Temp ©	Speed	Axil (x10)	Revs/Hr	
10/5/12	8:55 a.m.	38	19	2268626	-	Start
10/5/12	11:30 a.m.	39	19	-	-	
10/5/12	1:22 p.m.	39.8	19	2270919	286.625	Stop
10/5/12	1:37 p.m.	39.8	19	-	-	Start
10/5/12	5:30 p.m.	40.4	19	227062	285.75	Stop

Bio Asphalt Slab Cycles

Date	Time	HMA Temp ©	Speed	Axil (x10)	Revolutions/Hr	
12/7/12	8:15 AM	36.2	19.1	2389284	287	Start
12/7/12	11:15 AM	38	19.1	2390145	282.2	
12/7/12	4:15 PM	38.8	19.1	2391556	284	Stop

9.3 Fatigue Analysis

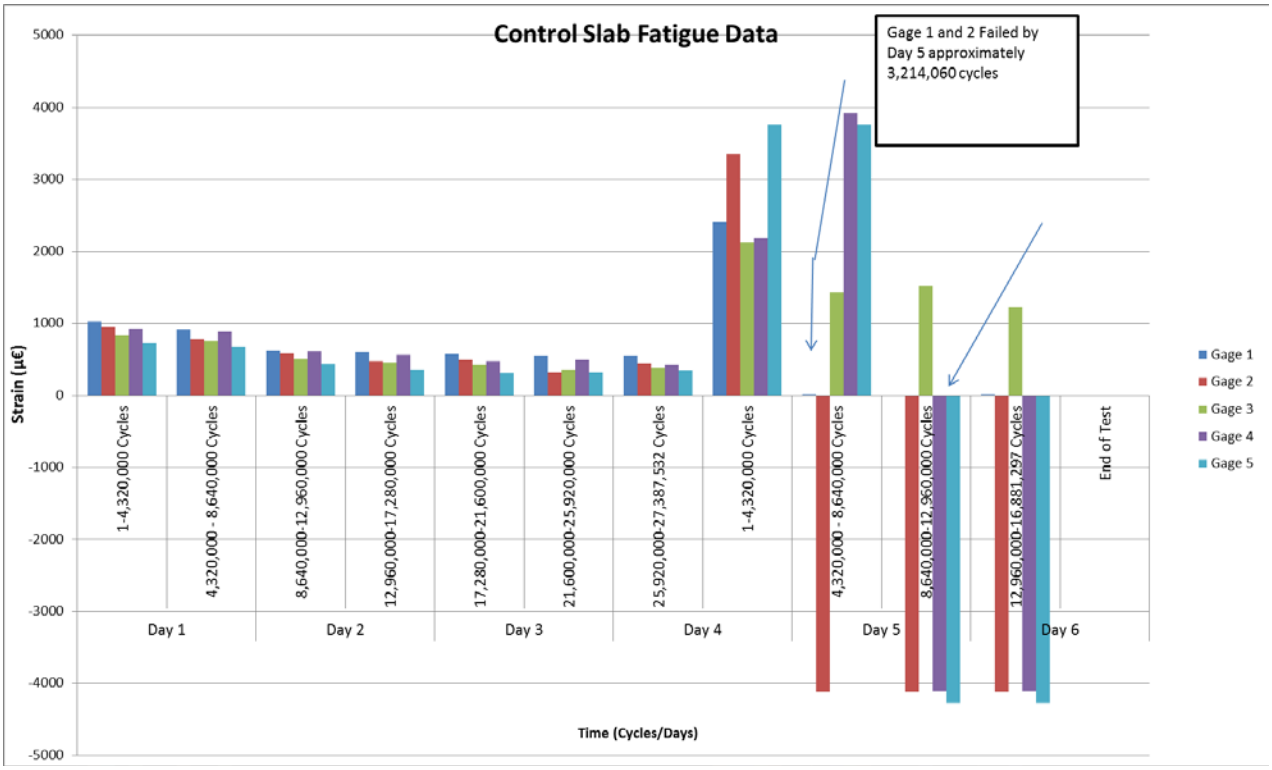

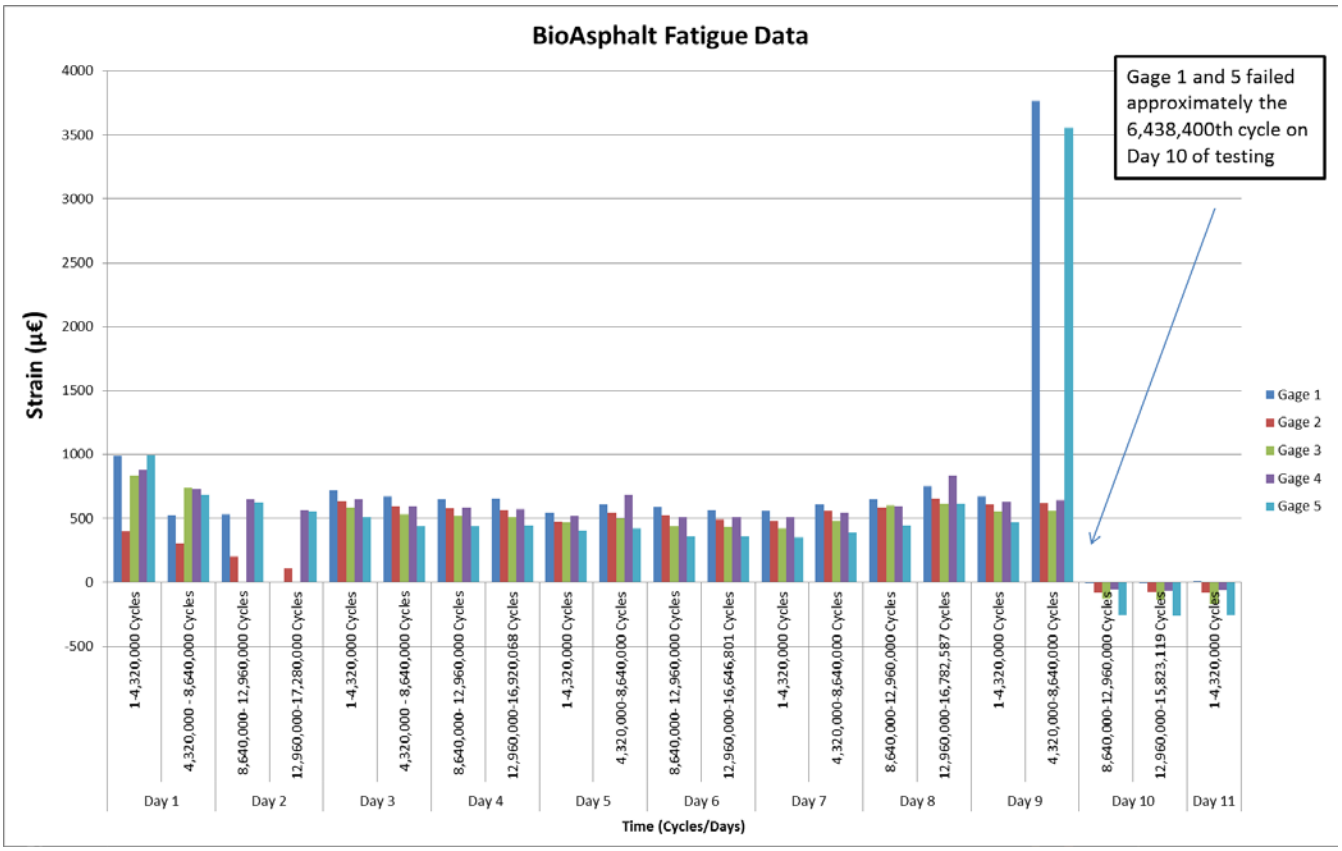

MatLAb Code; Control Slab Strain Readings

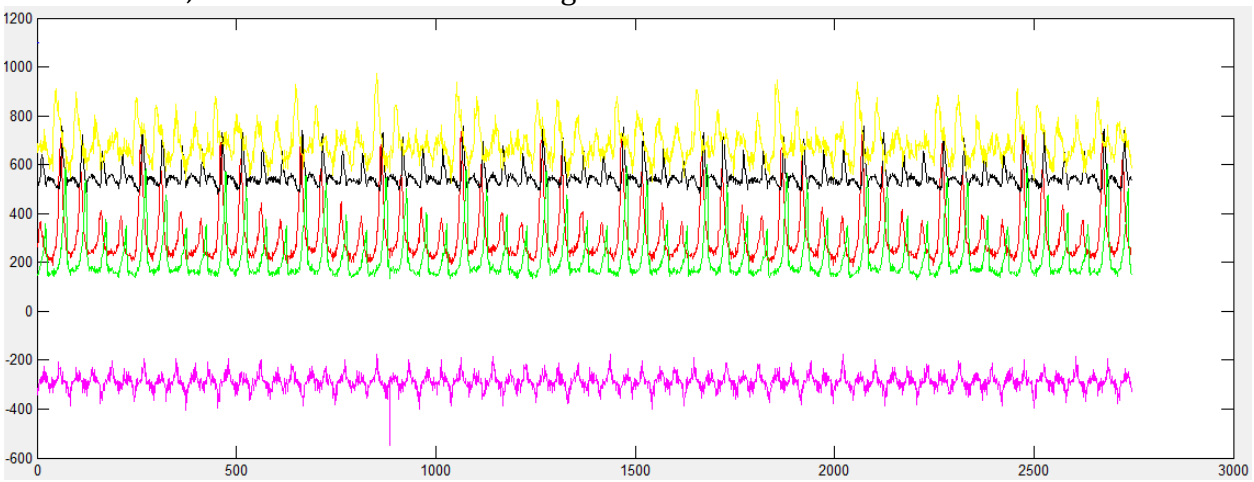

MatLab Code; Control Slab Strain Failure Readings

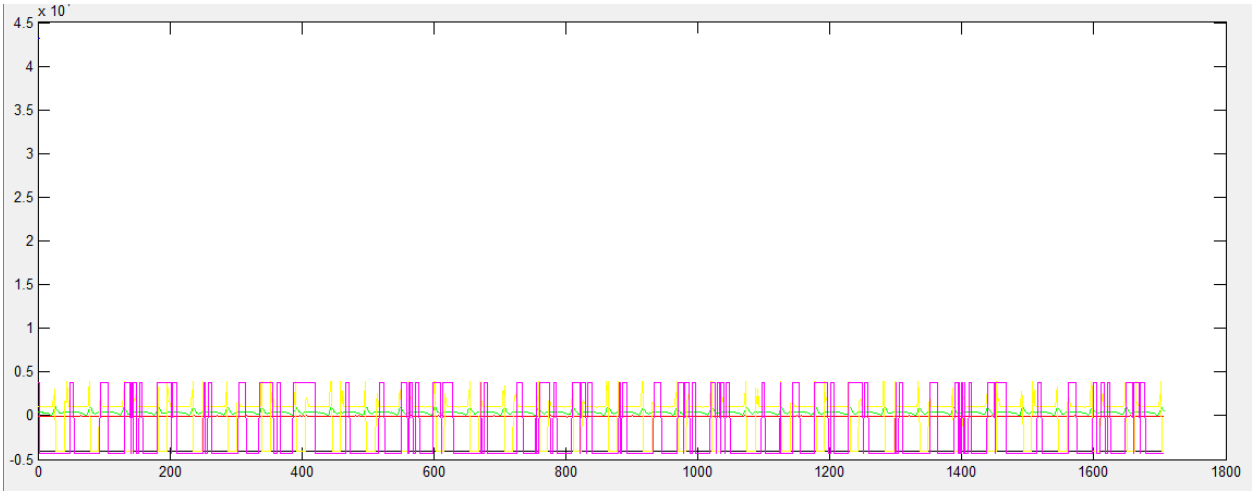

MatLab Code; Bio Asphalt Slab Strain Readings

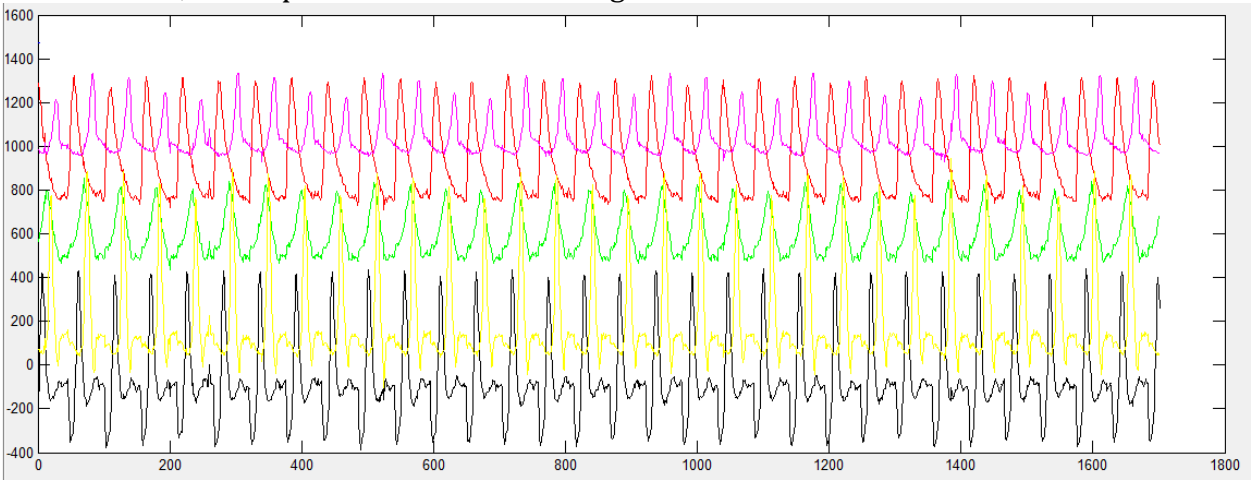

MatLab Code; Bio Asphalt Slab Strain Failure Readings